Reports

Digital PCR to determine the number of transcripts from single neurons after patch-clamp recording

Nóra Faragó[1,2,*], Ágnes K. Kocsis[3*], Sándor Lovas[3], Gábor Molnár[3], Eszter Boldog[3], Márton Rózsa[3], Viktor Szemenyei[3], Enikő Vámos[3], Lajos I. Nagy[1], Gábor Tamás[3], and László G. Puskás[1,2]

[1]Avidin Ltd., Szeged, Hungary, [2]Laboratory for Functional Genomics, Department of Genetics, Biological Research Center, Hungarian Academy of Sciences, Szeged, Hungary, and [3]Research Group for Cortical Microcircuits of the Hungarian Academy of Sciences Department of Physiology, Anatomy and Neuroscience, University of Szeged, Hungary

BioTechniques 54:327-336 (June 2013) doi 10.2144/000114029

Keywords: Digital PCR; single cell PCR; patch-clamp recording; gene expression

Supplementary material for this article is available at www.BioTechniques.com/article/114029

*N.F. and A.K.K contributed equally to this work.

Whole-cell patch-clamp recording enables detection of electrophysiological signals from single neurons as well as harvesting of perisomatic RNA through the patch pipette for subsequent gene expression analysis. Amplification and profiling of RNA with traditional quantitative real-time PCR (qRT-PCR) do not provide exact quantitation due to experimental variation caused by the limited amount of nucleic acid in a single cell. Here we describe a protocol for quantifying mRNA or miRNA expression in individual neurons after patch-clamp recording using high-density nanocapillary digital PCR (dPCR). Expression of a known cell-type dependent marker gene (*gabrd*), as well as oxidative-stress related induction of *hspb1* and *hmox1* expression, was quantified in individual neurogliaform and pyramidal cells, respectively. The miRNA *mir-132*, which plays a role in neurodevelopment, was found to be equally expressed in three different types of neurons. The accuracy and sensitivity of this method were further validated using synthetic spike-in templates and by detecting genes with very low levels of expression.

Gene expression analyses typically require RNA from thousands of cells, but neurons of specific types cannot be isolated in such large quantities. Population-average expression profiling of multiple neurons provides an incomplete picture, masking transcription patterns of individual cells that reflect physiological roles in the brain, activation state, or disease phenotype in a complex microcircuit (1–2). In this context, transcription profiling from whole brain tissue or populations of neurons isolated by fluorescence activated cell sorting (FACS) with specific antibodies cannot fully relate expression changes to a certain cell type or distinguish cell specific patterns (3–4). This is also the case for laser capture microdissection where the selection criteria are based on cellular morphology (5).

To determine physiological relationships within complex neuronal microenvironments in single, live neurons, whole-cell patch-clamp recording is an optimal approach. When coupled with gene expression analysis from the same cell, it provides a better understanding of how changes at the molecular level are manifested at the level of cell function and also enables better classification of different neuron types (6–7). After whole-cell patch-clamp recording of electrophysiological signals from single neurons, RNA from the perisomatic region can be harvested through the patch pipette. Linear (6) or exponential (PCR based) (7) amplification techniques can then be used to analyze expression of individual genes. Lambolez and colleagues were the first to combine patch-clamp recordings with PCR-based gene expression analysis of single neurons in culture (7). Using targeted preamplification and subsequent quantitative real-time PCR (qRT-PCR), one can detect tens or hundreds of mRNA or miRNA molecules(8). In principle, this approach can be also applied to RNA harvested from patch-clamped cells.

When faced with sensitivity concerns related to single cell qRT-PCR, digital PCR (dPCR) is a logical alternative (9–11). In

Method summary:

We present an approach for determining exact mRNA or miRNA copy numbers in single neurons after patch-clamp recording by using high-density nanocapillary digital PCR technology. This method can identify individual genes participating in the establishment and maintenance of particular neuronal phenotypes, deconvolve different neuronal cell types, and determine the exact distribution or variability of gene expression profiles for electrophysiologically phenotyped cells more precisely than classical single cell qPCR.

dPCR, single cDNA molecules are amplified in subreactions to generate binary calls. When cDNA molecules are partitioned evenly among hundreds of individual reactions, an absolute readout of total DNA copy number can be obtained. By generating thousands of subreactions on nanofluidic arrays, digital arrays represent the most powerful solution for high-throughput qRT-PCR and dPCR measurements (12–16).

Here we present the first report of the combination of dPCR, using the OpenArray platform (Life Technologies, Carlsbad, CA), and patch-clamp techniques to assess mRNA and miRNA expression in single neurons. This opens the door to sophisticated gene expression and regulatory network analysis on electrophysiologically manipulated neuronal cells.

Table 1. Average copy number (dPCR) or C_T value (qRT-PCR) for genes from different neuron types

dPCR	NGFC	CV%	FSBC	CV%	PC	CV%	No template	CV%	*n*
rps18	67.67 (20.26)	30.4	59.43 (24.54)	41.3	60.25 (21.04)	34.9	0.63 (1.06)	168.2	7
gabrd	33.60 (0.89)	2.6	7.60 (4.28)	56.3	2.00 (1.22)	61.0	0.43 (0.53)	123.3	5
mir-132	25.80 (2.17)	8.4	23.00 (2.94)	12.8	25.60 (3.91)	15.3	1.67 (0.58)	34.7	5

qRT-PCR*	NGFC	CV%	FSBC	CV%	PC	CV%	No template	CV%	*n*
rps18	20.80 (1.71)	327.2	20.69 (1.85)	360.5	21.20 (2.32)	499.3	baseline	-	6
gabrd	23.32 (3.64)	1246	27.15 (4.34)	2025	baseline	-	baseline	-	2
mir-132	23.69 (2.32)	499.3	24.85 (0.91)	187.9	22.87 (2.35)	509.8	baseline	-	4

*C_T values after 15 pre-amplification cycles; STDEV in brackets.

Materials and methods

Electrophysiology

All procedures were conducted with the approval of the University of Szeged and in accordance with the National Institutes of Health Guide to the Care and Use of Laboratory Animals. Wistar male rats (P22–40) were anesthetized by intraperitoneal injection of ketamine (30 mg/kg) and xylazine (10 mg/kg). Following decapitation, coronal slices (350 µm thick) were prepared from the somatosensory cortex. Slices were incubated at room temperature for 1 h in artificial cerebrospinal fluid (130 mM NaCl, 3.5 mM KCl, 1 mM NaH_2PO_4, 24 mM $NaHCO_3$, 1 mM CaCl, 3 mM $MgSO_4$, 10 mM D(+)-glucose) saturated with 95% O_2 and 5% CO_2. The solution used during recordings differed only in that 3 mM $CaCl_2$ and 1.5 mM $MgSO_4$ were used (17). In an oxidative stress model experiment, hydrogen peroxide (0.3 mM final concentration) was added to the artificial cerebrospinal fluid and applied to cortical slice preparations for 2 h. All other procedures were conducted with the same protocol. Micropipettes (5–7 MΩ) were filled with intracellular solution (126 mM K-gluconate, 4 mM KCl, 10 mM HEPES, 10 mM creatine phosphate, 8 mM biocytin; pH 7.25; 300 mOsm) supplemented with RNase Inhibitor (1U/µl, Life Technologies) to prevent any RNA degradation. Somatic whole-cell recordings were obtained at ~36°C from neurogliaform cells, pyramidal cells, and fast spiking interneurons. Cells were visualized by infrared differential interference contrast videomicroscopy (Axioskop microscope, Carl Zeiss, Oberkochen, Germany; CCD camera, Hamamatsu, Tokyo, Japan; Infrapatch set-up, Luigs & Neumann, Ratingen, Germany; two HEKA EPC 9 Double patch-clamp amplifiers, Lambrecht, Pfalz, Germany). Signals were filtered at 5 kHz, digitized at 10 kHz, and analyzed with PULSE software (HEKA, Lambrech/Pfalz, Germany). We identified the recorded cells by their membrane and firing characteristics (18) and also with post hoc light microscopic assessment.

Single cell harvesting

At the end of recording, as much of the intracellular content as possible was aspirated into the recording pipette by application of a gentle negative pressure while maintaining the tight seal. The pipette was then delicately removed to allow outside-out patch formation (19). Next, the content of the pipette (2 µl) was expelled into a low-adsorbtion test tube (Axygen, Tewksbury, MA). The sample was snap-frozen in liquid nitrogen and stored or immediately used for reverse transcription (RT).

First-strand cDNA synthesis of mRNA

RT was carried out in two steps. The first step was done for 5 min at 65°C in a total reaction volume of 5 µL, containing 2 µL intracellular solution with the cytoplasmic contents of the neuron, 0.3 µL reverse primer (Bioneer Corporation, Daedong, Korea), 0.3 µL 10 mM dNTPs (Life Technologies, Foster City, CA), 1 µL 5X first-strand buffer, 0.3 µL 0.1 mol/L DTT, 0.3 µL RNase inhibitor (Life Technologies) and 100 U of reverse transcriptase (Superscript III, Invitrogen, Carlsbad, CA). RT primers were designed using the CLC Main Workbench (CLC Bio, Aarhus, Denmark) software. RT primer sequences were:

rps18
5′-ATTAACAGCAAAGGCCCA-3′

gabrd
5′-CCCCTACTCTCTTTCTCT-3′

hspb1
5′-CAGGGAAGAGGACACCAA-3′

hmox1
5′-GAGAGACAAAGGAAGACA-3′

The second step of the reaction was carried out at 50°C for 1 h and then the reaction was stopped by heating at 70°C for 15 min. The RT reaction mix was stored at -20°C until PCR amplification.

First-strand cDNA synthesis of miRNA

RT was performed using the TaqMan MicroRNA Reverse Transcription Kit (Life Technologies). The miRNA from each individual cell was reverse transcribed in the presence of TaqMan MicroRNA Assays (Life Technologies). Seven µl reaction mixtures contained 0.2 µl dNTPs, 1 µl MultiScribe Reverse Transcriptase (50 U/µL), 1.5 µl 10X RT Buffer, 0.2 µl RNase Inhibitor (20 U/µL), 1.5 µl 5X RT primer, 0.6 µl nuclease-free water, and the template, for a total volume of 2 µl. RT was carried out with the following cycling parameters in a thermocycler (MyGenie; Bioneer): 16°C for 2 min, 42°C for 1 min, 50°C for 1 s, 45 cycles, then the samples were held at 85°C for 5 min.

Single cell qRT-PCR

Traditional single cell qRT-PCR was carried out after preamplification of cDNA in a total volume of 20 µl (5 µL RT product, 1 µL TaqMan primer (*rps18*: Rn01428913_gH; *gabrd*: Rn01517017_g1; *hsa-miR-132*: 000457), 10 µL TaqMan PreAmp Master Mix (Life Technologies) and 4.5 µL nuclease-free water) in a MyGenie 32 Thermal Block (Bioneer) with the following cycling protocol: 10 min hot start at 95°C, 2 min at 55°C, 2 min at 72°C followed by 15 cycles (15 s at 95°C, 4 min at 60°C), and finally 10 min at 99°C for inactivation of the enzyme. After preamplification, qRT-PCR was carried out in an Exicycler 96 (Bioneer) in a total volume of 20 µL containing 1.5 µL preamplified PCR mixture, 1 µL TaqMan primer and 10 µL FastStart TaqMan Probe Master (Roche Diagnostics GmbH, Mannheim, Germany). The following protocol was used: 3 min at 95°C followed by 45 cycles (40 s at 95°C, 40 s at 56°C, and 1 min at 72°C). The Exicycler 96 Analysis Software (Bioneer) determined a cycle threshold (C_T) value, which identified the first cycle at which the fluorescence was detected above the baseline for that sample. For each gene, average threshold cycle (C_T) values were presented (Table 1).

Digital PCR

For dPCR analysis, half (2.5 µL, in the case of *rps18*) or all (for all other genes) of the RT reaction mixture having different numbers of synthetic spike-in templates (*s_rps18*: 5′- TGTGCCGCCGCCATGTCCCTAGTGATCCCCGAGAAGTTTCAGCACATCCTGCGAGTACTCAACACC-3′), 2 µL TaqMan Assays (inventoried, *hspb1*: Rn00583001_g1; *hmox1*: Rn01536933_m1; *slc2a4*: Rn01752377_m1; see other probes above; Life Technologies), 10 µL OpenArray Digital PCR Master Mix (Life Technologies) and nuclease free water (2–4.5 µL) were mixed in a total volume of 20 µL. The mixture was evenly distributed on an OpenArray plate. RT mixes were loaded into 4 wells of a 384-well plate from which the OpenArray autoloader transferred the cDNA master mix by capillary action into 256 nanocapillary holes (4 subarrays) on an OpenArray plate. Processing of the OpenArray slide and cycling in the OpenArray NT cycler were done as previously described (12, 16). Data analysis was performed using the Biotrove OpenArray Digital PCR Software version 1.0 (download at www.appliedbiosystems.com / Support / OpenArray Digital PCR Software), which uses a proprietary calling algorithm to estimate the quality of each individual threshold cycle (C_T) value by calculating a C_T confidence value for the amplification reaction. For our dPCR protocol amplification, reactions with C_T confidence values below 100 as well as reactions having C_T values less than 23 or greater than 33 were considered primer dimers or background signals, respectively, and excluded from the data set. Statistical analysis of expression data from hydrogen peroxide treated cells was performed with an unpaired *t*-test.

Sequencing

We sequenced PCR products from individual neurogliaform and pyramidal cells using capillary electrophoresis sequencing on a 3500 Genetic Analyzer (Life Technologies). After single cell PCR, we reamplified 10 µl of the reaction mixture with primers having a universal sequencing tag at the 5′-end of the forward primers and an opseq sequencing tag at the 5′-end of the reverse primers (see italicized letters in the sequences) with the following primers:

rps18
Forward: 5′-GCCAGGGTTTTCCCAGTCACGACACGCCGCCGCTTGTGCC-3′
Reverse: 5′-TGTGTGGAATTGTGAGCGGTGGTGTTGAGTACTCGCAGG-3′

gabrd
Forward: 5′-GCCAGGGTTTTCCCAGTCACGACAAGGTCACGAAGCCAAGG-3′
Reverse: 5′-TGTGTGGAATTGTGAGCGGGCAGCAGAGAGGGAGAAGAG-3′

hspb
Forward: 5′-GCCAGGGTTTTCCCAGTCACGAGGATGAACATGGCTACATCTC-3′
Reverse: 5′-TGTGTGGAATTGTGAGCGGCACCGTGAGTGTGCCCTCAG-3′

hmox-1
Forward: 5′-GCCAGGGTTTTCCCAGTCACGAGGGTGACAGAAGAGGCTAAG-3′
Reverse: 5′-TGTGTGGAATTGTGAGCGGGACTCTGGTCTTTGTGTTCC-3′

slc2a4
Forward:5′-CCGTCGGGTTTCCAGCAG-3′
Reverse: 5′-CAGCAAGGACCAGTGTCCCAG-3′

After purification of the products, we used different universal and opseq sequencing primers. Sequence homology searches were performed using the BLASTN algorithm (www.ncbi.nlm.nih.gov/Blast.cgi).

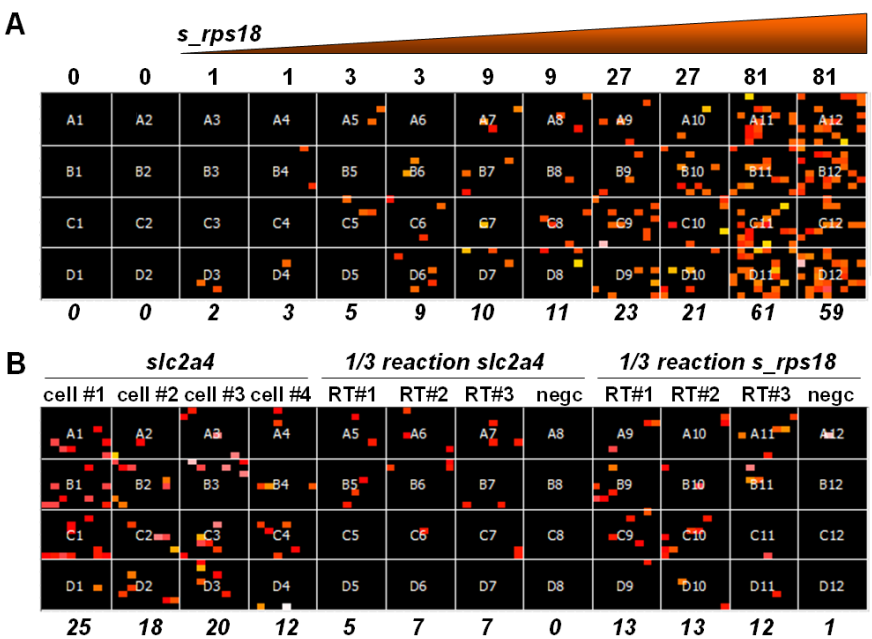

Figure 1. Application of spike-in templates for dPCR analysis. (A) Synthetic *rps18* templates (*s_rps18*) diluted to a range of 0–81 copies per reaction (see values above the picture, n = 2) was analyzed using the Openarray dPCR platform. Resulting positive calls are represented by orange or red dots (values are shown below the picture). (B) dPCR amplification of *slc2a4* was carried out either with the entire cellular contents of one cell (cell#1-cell#4, n = 4) or one third of a single cell RT reaction volume (RT#1-RT#3, n = 3). Spike-in *s_rps18* dPCR amplification were done from the same single cell RT reaction from which *slc2a4* was amplified (RT#1-RT#3, n = 3). The number of positive reactions from individual dPCRs are shown below the picture. The negative control is labled negc.

Results and discussion

Analysis of serial dilution of spike-in templates with dPCR

To circumvent the sensitivity issues associated with single cell qRT-PCR, we used high-throughput nanocapillary qRT-PCR to record digital signals from mRNA isolated from a single cell in a dPCR setup. To verify sensitivity and dynamic range, we recorded the presence of individual, synthetic target molecules (*s_rps18* having the amplicon sequence of rat *rps18*) in a serial dilution study. Synthetic *rps18* template was diluted in parallel experiments (n = 2) to obtain 1–81 molecules in individual reaction mixes containing TaqMan probes for the *rps18* gene. The mixtures were partitioned evenly among hundreds of individual reactions and an absolute readout of total copy number was obtained after qRT-PCR in the OpenArray plate format. The through-hole nanofluidic arrays on the OpenArray plates consist of 3200 subreactions in a 48 subarray format (12, 16). In our study, we divided the plates into 12 sections, each possessing 4 subarrays and 256 individual reactions with different numbers of *rps18* template copies compared to a no template negative control. After dPCR, pictures were generated using the OpenArray Digital Software (Life Technologies). We obtained good correlation between the theoretically calculated numbers of template molecules in the reaction mixture and the number of positive hits (Figure 1). Moderate differences at the lower end (less than nine molecules) of the dilution spectrum were likely caused by pipetting errors or variability in the spectrophotometric measurements used in the calculations. More pronounced differences at the higher end (more than 27 molecules) of the

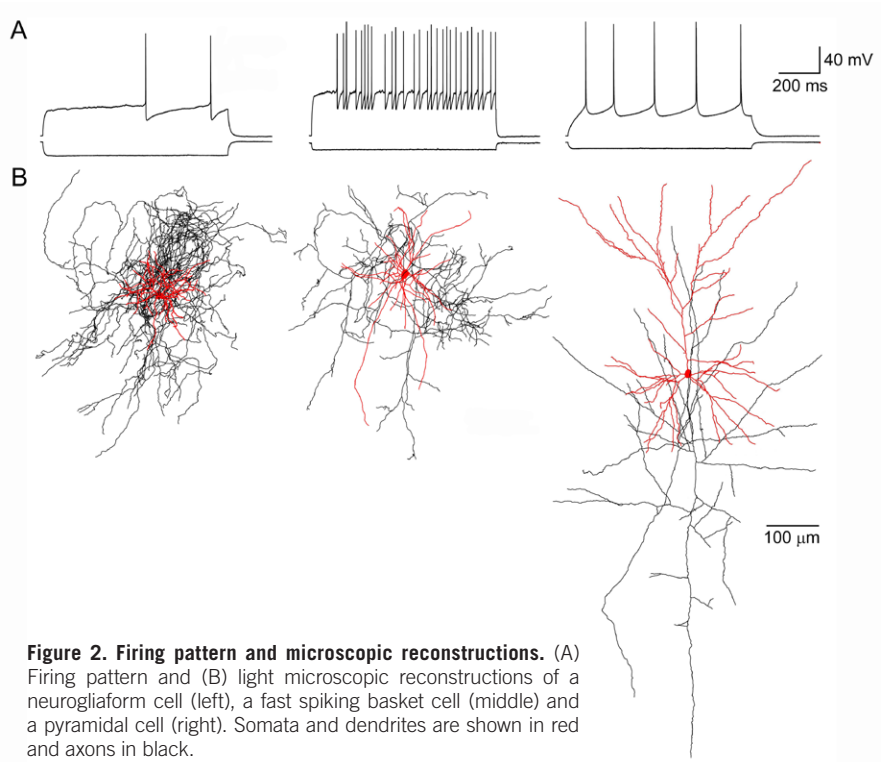

Figure 2. Firing pattern and microscopic reconstructions. (A) Firing pattern and (B) light microscopic reconstructions of a neurogliaform cell (left), a fast spiking basket cell (middle) and a pyramidal cell (right). Somata and dendrites are shown in red and axons in black.

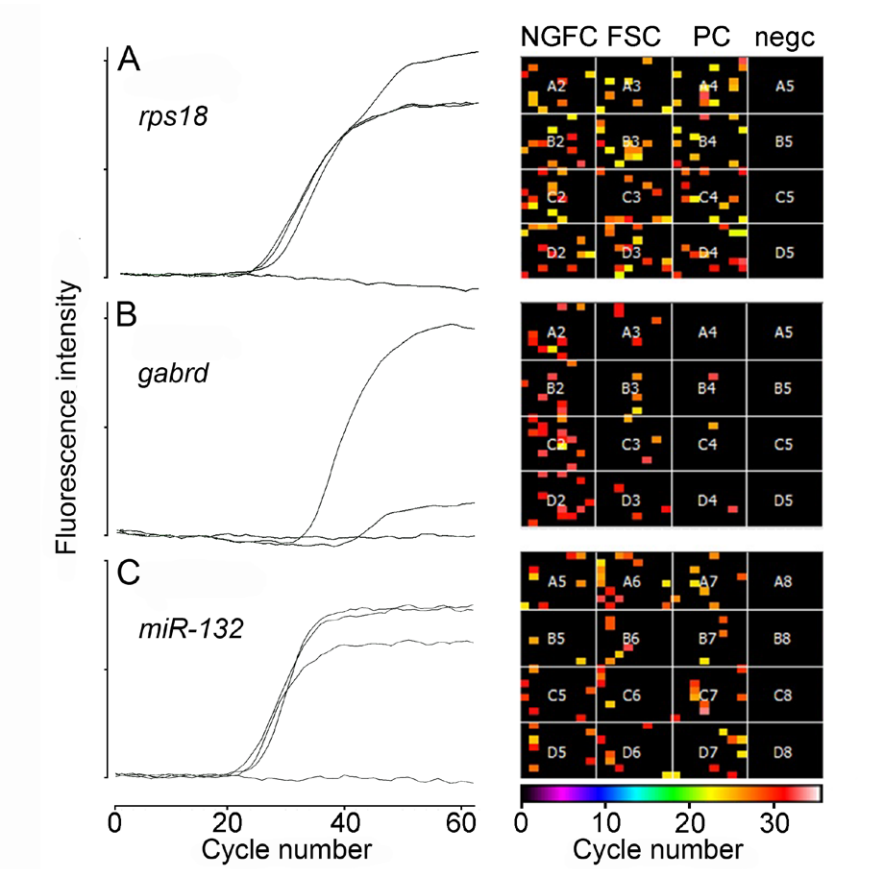

Figure 3. mRNA and miRNA expression in different neuron types. Expression of *rps18*, *gabrd*, and *mir-132* in neurogliaform cells (NGFC), fast-spiking basket cells (FSC), and pyramidal cells (PC). No template controls (negc) from the cerebral cortex were determined by single cell QRT-PCR or dPCR.

dilution spectrum can be explained by the presence of more than 1 template molecule per nanoliter volume reaction. Therefore, if more than 30 cDNA copies per sample are present in 1 cell, the samples should be diluted or evenly distributed among 512 or more individual subreactions.

mRNA expression analysis of single neurons with dPCR

With a similar experimental setup (see the flowchart of the dPCR protocol in Supplementary Figure S1), we were able to detect individual genes from single neurons after patch-clamp recording. The cellular content of an individual neuron was aspirated into the recording pipette and expelled directly into a low-adsorbtion test tube containing first strand cDNA synthesis buffer with RNase inhibitor to prevent RNA degradation. RT reactions were performed with RT primers for the gene of interest and extracts from individual cells. Subsequently, the RT reaction mixture, TaqMan probes, and qRT-PCR reagents were mixed and evenly distributed among the 256 (4 subarrays) nanocapillary holes on an OpenArray plate.

The expression of *slc2a4* (GLUT4) was analyzed in individual neurogliaform cells after patch-clamp recording and was found to have 12–25 (18.75 ± 5.38) copies per cell (n = 4) (Figure 1B). In order to demonstrate reproducibility and sensitivity, 3 independent RT reactions were prepared with single cell aspirates and approximately similar numbers of copies (24 molecules) of the synthetic spike-in *rps18* templates (*s_rps18*) compared to the estimated number of *slc2a4* messages per cell (reaction mixtures: RT#1-RT#3). One-third of the RT mixture was applied to dPCR amplification of *slc2a4* and one-third from the same RT mixture to detect the number of *s_rps18* molecules (n = 3). Digital images as well as individual positive amplification reactions are shown in Figure 1B. An unexpectedly even representation of the *s_rps18* molecules (12, 13, and 13 copies) could be recorded in the 3 independent experiments, validating the reproducibility of our protocol. Moreover, when multiplying the identified *slc2a4* cDNA molecules by 3, we found an almost perfect match (17 ± 3.46, n = 3) with the results obtained from the non-diluted samples.

Cell-type specific mRNA expression analysis of single neurons with dPCR

In order to obtain cell-type specific mRNA expression data with our protocol, three extensively characterized cell types from the supragranular layers of the rat somatosensory cortex were selected. Whole cell recorded neurogliaform cells , fast spiking basket cells, and pyramidal cells were identified based on their late spiking, fast spiking, and regular spiking

responses to current pulses as well as their axonal and dendritic morphology (Figure 2) (20–24).

To demonstrate the utility, reproducibility, and sensitivity of our protocol, the expression of the housekeeping gene *rps18* and a potential cell-type dependent marker gene, gamma-aminobutyric acid (GABA) A receptor delta subunit (*gabrd*) were recorded by dPCR from individual cellular aspirates from the three different neuron types. After recording the firing pattern for each neuron (22), the cellular content was aspirated and used for cDNA synthesis. Five independent cells from each type were collected from three brain slices in separate experiments and measurements of transcript numbers for each gene were repeated five times in an independent assay. Transcript numbers for each cell are listed in Table 1.

The expression of *rps18* was found to be similar in each type of neuron (59–67 copies/cell), with low CV values (30%–40%) (Table 1). On average, only two *gabrd* mRNA copies could be detected in pyramidal cells (with a standard deviation of 1.22); a few transcripts were recorded in fast-spiking neurons (7.60 ± 4.28), representing *gabrd,* a specific gene with low expression levels, while over 30 messages could be recorded in neurogliaform cells (Table 1).

Cell-type specific miRNA expression analysis of single neurons with dPCR

To understand the role of miRNAs in different neuronal processes, including pathological alterations, there must be an understanding of how different miRNAs are expressed in different cell types. Multiplex miRNA expression profiles were determined in single cells with qRT-PCR (25). Recently, the applicability of the high-density OpenArray protocol has been demonstrated for the detection of miRNA expression profile by stem-looped RT-PCR (26). As a model, we used the OpenArray plates for dPCR studies of a specific miRNA, *mir-132,* from cytoplasm harvested into patch pipettes from single neurons of different types. Specific miRNA was converted into cDNA using specific stem-looped primers. The total RT reaction was amplified in 256 individual reaction holes on the array as described above. As an example, the number of *mir-132* molecules was determined in pyramidal cells, fast spiking cells, and neurogliaform interneurons. Dysregulation of *mir-132* has been found in schizophrenia and *mir*-132 is also involved in neurodevelopmental processes; however, there are only limited data on cell-type specific expression (27). By using our dPCR protocol, *mir-132* expression was found to be similar in the three cell types (Table 1, Figure 3), although differential expression cannot be excluded in these cells during different periods of neurodevelopment or under pathophysiological conditions.

In order to demonstrate the sensitivity of our protocol, a miRNA with low expression levels was selected for analysis in neurons. In our preliminary single cell qRT-PCR studies, we found that the expression of *mir-184* was very low or even undetectable by standard protocols in both neurogliaform and pyramidal cells (data not shown). By using our combined patch-clamp and dPCR approach, we detected an average of 2.33 ± 1.58 (n = 3) copies in pyramidal cells and 3.33 ± 1.52 (n = 3) copies in neurogliaform cells, while RT negative controls resulted in 0.33 ± 0.58 (n = 3) false positive calls.

Demonstration of specific mRNA and miRNA expression in single cells with traditional qRT-PCR

To confirm mRNA (*rps18* and *gabrd)* and miRNA (*mir-132*) expression in single neurons analyzed by our dPCR approach, classical single cell qRT-PCR was run on all three neuron types used in this study (Figure 3). Analysis of ΔC_T values obtained by classical single-cell qRT-PCR produced results corresponding to those obtained with dPCR for both mRNA and miRNA (Table 1). Expression of *gabrd* was specific to neurogliaform cells (average C_T value of 23.32), with significantly lower expression levels detected in fast spiking cells. No amplification was recorded in pyramidal cells.

CV values were determined for each neuron and each gene analyzed. We found that our dPCR protocol resulted in data with small CV (8%–60%), while CV values obtained from traditional PCR were high (187%–2025%), likely because of low quantities of input DNA in the reactions. From these data, we conclude that dPCR in combination with single cell patch-clamp technology enables absolute quantitation of transcript copy numbers in a reproducible manner.

Physiological alteration of gene expression in single neurons determined with dPCR

The approach described here can also be used to isolate and evaluate single abnormal neurons in various disease models of the central nervous system (CNS). In a model experiment, oxidative stress was introduced by applying hydrogen peroxide at a 0.3 mM final concentration onto cortical slice preparations submerged in artificial cerebrospinal fluid for 2 h. Pyramidal cells were harvested by patch-clamp from non-treated and hydrogen peroxide treated brain slices. dPCR of the samples was run on OpenArray plates to determine the relative mRNA copy number changes of *hmox1* and *hspb1* genes. Both genes have been implicated in oxidative stress and methamphetamine-induced neurotoxicity (28). We found that this short period of oxidative stress did not alter the number of the house-keeping *rps18* transcripts (P = 0.918), but significantly elevated the number of mRNA molecules of both *hmox1* and *hspb1* genes ($P < 0.05$; Table 2, Figure 4).

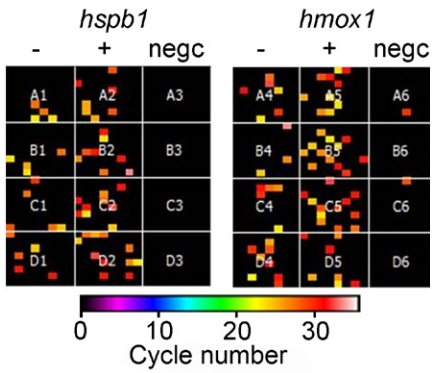

Figure 4. Oxidative-stress dependent expression changes. mRNA copy number changes of *hmox1* and *hspb1* in pyramidal cells. Results of no template controls for all the genes analyzed with dPCR (negc) are also shown.

Demonstration of specific amplification during PCR

To demonstrate the specificity of TaqMan probes used in single cell qRT-PCR as well as in dPCR, control parameters were tested including a reverse transcription negative control (where all the reagents except the RT reaction mix were applied), intronic template DNA, and intergenic template DNA. These reactions resulted in no amplification with qRT-PCR and few or no amplification products (maximum of 2) with dPCR (Table 1).

To determine the background noise for *gabrd,* we repeated the amplification of the negative control reaction 7 times and found an average of 0.43 signals with a standard deviation of 0.53.

To eliminate the possibility of amplifying genomic DNA, we tried to amplify multiple introns of the *ins2* gene as well as an intergenic region at the *ifngr1* gene locus on chromosome 1. None of these primer sets gave positive

Table 2. mRNA average copy numbers of untreated and H_2O_2-treated pyramidal cells (PC).

dPCR	PC	Pc + H202	No template	*n*	*P* value
rps18	60.25 (21.04)	63.33 (11.37)	0.63 (1.06)	7	0.918
hmox1	18.00 (3.00)	29.25 (3.59)	0.50 0.71)	4	0.007
hspb1	24.00 (4.36)	38.5 (6.45)	0.00 (0.00)	4	0.02

results during qRT-PCR or dPCR, meaning that no genomic amplification occurred during our study (data not shown).

To demonstrate that single cell qRT-PCR resulted in the desired PCR fragments, we sequenced PCR products from individual neurogliaform and pyramidal cells. Although we used validated TaqMan probes in the present study, we sequenced PCR products for all of the amplified genes. Using BLASTN homology searches, we found a 100% match to each gene sequence (data not shown). These data confirm that minimal to no amplification of genomic DNA occurred and that amplifications were highly specific.

Strengths and limitations

One of the strengths of our PCR protocol compared to other end-point amplification based PCR methods is that the detection of positive signals is based on individual real-time PCR read-outs. By using the calling algorithm in the OpenArray software and having different thresholds for C_T confidence intervals and cycle cutoff values, most of the false positive hits generated by primer dimers or nonspecific amplifications can be excluded.

Partitioning the sample into hundreds or thousands of independent reaction holes (in the case of OpenArray plates) or reaction chambers (using the Fluidigm technology) during dPCR increases the detection sensitivity of specific DNA molecules by increasing the target-to-background ratios (12,14,16).

Here we described the combination of whole-cell patch-clamp recording with digital analysis of specific mRNA or miRNA using high-density nanocapillary dPCR. The accuracy and sensitivity of the method was validated with spike-in templates as well as by detecting cDNA from genes with low levels of expression. One of the main advantages of this approach is that accurate digital gene expression analyses can be performed on electrophysiologically defined single neurons. The real-time PCR based dPCR protocol, along with the application of different thresholds for confidence C_T and cycle cutoff values led to low rates of false positive calls. However, the limitations of the technique are the relative high cost per sample and low-throughput, which restricts the number of genes that can be analyzed from the same cell.

Acknowledgments

This work was supported by the following grants: ERC Advanced Grant, EURYI, NIH N535915 and the Hungarian Academy of Sciences (G.T.), and GOP-1.1.1-11-2011-0003 from the National Investment Agency (NIH) (Avidin, BRC).

Competing interests

The authors declare no competing interests.

References

1. **Monyer, H. and B. Lambolez.** 1995. Molecular biology and physiology at the single-cell level. Curr. Opin. Neurobiol. *5*:382-387.
2. **Sugino, K., C.M. Hempel, M.N. Miller, A.M. Hattox, P. Shapiro, C. Wu, Z.J. Huang, and S.B. Nelson.** 2006. Molecular taxonomy of major neuronal classes in the adult mouse forebrain. Nat. Neurosci. *9*:99-107.
3. **Hinkle, D., J. Glanzer, A. Sarabi, T. Pajunen, J. Zielinski, B. Belt, K. Miyashiro, T. McIntosh, and J. Eberwine.** 2004. Single neurons as experimental systems in molecular biology. Prog. Neurobiol. *72*:129-142.
4. **Ståhlberg, A., D. Andersson, J. Aurelius, M. Faiz, M. Pekna, M. Kubista, and M. Pekny.** 2011. Defining cell populations with single-cell gene expression profiling: correlations and identification of astrocyte subpopulations. Nucleic Acids Res. *39*:e24.
5. **Gründemann, J., F. Schlaudraff, O. Haeckel, and B. Liss.** 2008. Elevated alpha-synuclein mRNA levels in individual UV-laser-microdissected dopaminergic substantia nigra neurons in idiopathic Parkinson's disease. Nucleic Acids Res. *36*:e38.
6. **Eberwine, J., H. Yeh, K. Miyashiro, Y. Cao, S. Nair, R. Finnell, M. Zettel, and P. Coleman.** 1992. Analysis of gene expression in single live neurons. Proc. Natl. Acad. Sci. USA *89*:3010-3014.
7. **Lambolez, B., E. Audinat, P. Bochet, F. Crepel, and J. Rossier.** 1992. AMPA receptor subunits expressed by single Purkinje cells. Neuron *9*:247-258.
8. **Bengtsson, M., A. Stahlberg, P. Rorsman, and M. Kubista.** 2005. Gene expression profiling in single cells from the pancreatic islets of Langerhans reveals lognormal distribution of mRNA levels. Genome Res. *15*:1388-1392.
9. **Kalisky, T. and S.R. Quake.** 2011. Single-cell genomics. Nat. Methods *8*:311-314.
10. **Vogelstein, B. and K.W. Kinzler.** 1999. Digital PCR. Proc. Natl. Acad. Sci. USA *96*:9236-9241.
11. **Zeng, Y., R. Novak, J. Shuga, M.T. Smith, and R.A. Mathies.** 2010. High-performance single cell genetic analysis using microfluidic emulsion generator arrays. Anal. Chem. *82*:3183-3190.
12. **Fabian, G., N. Farago, L.Z. Feher, L.I. Nagy, S. Kulin, K. Kitajka, T. Bito, V. Tubak, et al.** 2011. High-Density Real-Time PCR-Based in Vivo Toxicogenomic Screen to Predict Organ-Specific Toxicity. Int. J. Mol. Sci. *12*:6116-6134.
13. **Morrison, T., J. Hurley, J. Garcia, K. Yoder, A. Katz, D. Roberts, J. Cho, T. Kanigan, et al.** 2006. Nanoliter high throughput quantitative PCR. Nucleic Acids Res. *34*:e123.
14. **Oehler, V.G., J. Qin, R. Ramakrishnan, G. Facer, S. Ananthnarayan, C. Cummings, M. Deininger, N. Shah, et al.** 2009. Absolute quantitative detection of ABL tyrosine kinase domain point mutations in chronic myeloid leukemia using a novel nanofluidic platform and mutation-specific PCR. Leukemia *23*:396-399.
15. **Spurgeon, S.L., R.C. Jones, and R. Ramakrishnan.** 2008. High throughput gene expression measurement with real time PCR in a microfluidic dynamic array. PloS One *3*:e1662.
16. **Vass, L., J.Z. Kelemen, L.Z. Feher, Z. Lorincz, S. Kulin, S. Cseh, G. Dorman, and L.G. Puskas.** 2009. Toxicogenomics screening of small molecules using high-density, nanocapillary real-time PCR. Int. J. Mol. Med. *23*:65-74.
17. **Oláh, S., M. Fule, G. Komlosi, C. Varga, R. Baldi, P. Barzo, and G. Tamas.** 2009. Regulation of cortical microcircuits by unitary GABA-mediated volume transmission. Nature *461*:1278-1281.
18. **Cauli, B., J.T. Porter, K. Tsuzuki, B. Lambolez, J. Rossier, B. Quenet, and E. Audinat.** 2000. Classification of fusiform neocortical interneurons based on unsupervised clustering. Proc. Natl. Acad. Sci. USA *97*:6144-6149.
19. **Ferezou, I., S. Bolea, and C.C. Petersen.** 2006. Visualizing the cortical representation of whisker touch: voltage-sensitive dye imaging in freely moving mice. Neuron *50*:617-629.
20. **Hestrin, S. and W.E. Armstrong.** 1996. Morphology and physiology of cortical neurons in layer I. J. Neurosci. *16*:5290-5300.
21. **Kawaguchi, Y.** 1995. Physiological subgroups of nonpyramidal cells with specific morphological characteristics in layer II/III of rat frontal cortex. J. Neurosci. *15*:2638-2655.
22. **Price, C.J., B. Cauli, E.R. Kovacs, A. Kulik, B. Lambolez, R. Shigemoto, and M. Capogna.** 2005. Neurogliaform neurons form a novel inhibitory network in the hippocampal CA1 area. J. Neurosci. *25*:6775-6786.
23. **Tamás, G., A. Lorincz, A. Simon, and J. Szabadics.** 2003. Identified sources and targets of slow inhibition in the neocortex. Science *299*:1902-1905.
24. **Zsiros, V. and G. Maccaferri.** 2005. Electrical coupling between interneurons with different excitable properties in the stratum lacunosum-moleculare of the juvenile CA1 rat hippocampus. J. Neurosci. *25*:8686-8695.
25. **Tang, F., P. Hajkova, S.C. Barton, D. O'Carroll, C. Lee, K. Lao, and M.A. Surani.** 2006. 220-plex microRNA expression profile of a single cell. Nat. Protoc. *1*:1154-1159.
26. **Grigorenko, E.V., E. Ortenberg, J. Hurley, A. Bond, and K. Munnelly.** 2011. miRNA profiling on high-throughput OpenArray system. Methods Mol. Biol. *676*:101-110.
27. **Miller, B.H. and C. Wahlestedt.** 2010. MicroRNA dysregulation in psychiatric disease. Brain Res. *1338*:89-99.
28. **Cadet, J.L., C. Brannock, B. Ladenheim, M.T. McCoy, G. Beauvais, A.B. Hodges, E. Lehrmann, W.H. Wood, et al.** 2011. Methamphetamine preconditioning causes differential changes in striatal transcriptional responses to large doses of the drug. Dose Response. *9*:165-181.

Received 07 January 2013; accepted 24 April 2013.

Address correspondence to László G. Puskás, Avidin Ltd., Szeged, Hungary. E-mail: laszlo@avidinbiotech.com or to Gabor Tamás, Research Group for Cortical Microcircuits of the Hungarian Academy of Sciences Department of Physiology, Anatomy and Neuroscience, University of Szeged, Hungary. E-mail: gtamas@bio.u-szeged.hu.